

A Stellar-mass Black Hole in the Ultra-luminous X-ray Source M82 X-1?

Takashi Okajima¹

*Code 662, Astrophysics Science Division, NASA's Goddard Space Flight Center, Greenbelt,
MD 20771*

Ken Ebisawa

*Institute of Space and Astronautical Science, 3-1-1 Yoshinodai, Sagamihara, Kanagawa,
229-8510, Japan*

and

Toshihiro Kawaguchi

*Department of Physics and Mathematics, Aoyama Gakuin University, Fuchinobe 5-10-1,
Sagamihara, Kanagawa 229-8558, Japan*

ABSTRACT

We have analyzed the archival *XMM-Newton* data of the bright Ultra-Luminous X-ray Source (ULX) M82 X-1 with an 105 ksec exposure when the source was in the steady state. Thanks to the high photon statistics from the large effective area and long exposure, we were able to discriminate different X-ray continuum spectral models. Neither the standard accretion disk model (where the radial dependency of the disk effective temperature is $T(r) \propto r^{-3/4}$) nor a power-law model gives a satisfactory fit. In fact, observed curvature of the M82 X-1 spectrum was just between those of the two models. When the exponent of the radial dependence (p in $T(r) \propto r^{-p}$) of the disk temperature is allowed to be free, we obtained $p = 0.61_{-0.02}^{+0.03}$. Such a reduction of p from the standard value $3/4$ under extremely high mass accretion rates is predicted from the accretion disk theory as a consequence of the radial energy advection. Thus, the accretion disk in M82 X-1 is considered to be in the *Slim disk* state, where an optically thick Advection Dominant Accretion Flow (ADAF) is taking place. We have applied a theoretical slim disk spectral model to M82 X-1, and

¹Department of Physics and Astronomy, The Johns Hopkins University

estimated the black hole mass $\approx 19 - 32M_{\odot}$. We propose that M82 X-1 is a relatively massive stellar black hole which has been produced through evolution of an extremely massive star, shining at a super-Eddington luminosity by several times the Eddington limit.

Subject headings: accretion, accretion disks — black hole physics — X-rays: individual (M82 X-1)

1. Introduction

Ultra-luminous X-ray Sources (ULXs) in nearby galaxies have typical X-ray luminosities from 10^{39} to 10^{41} erg s^{-1} (e.g., Makishima et al. 2000; Ptak & Colbert et al. 2004). M82 X-1 is the most luminous ULX which is located off the nucleus of the galaxy and has exhibited X-ray flares as bright as $\sim 10^{41}$ erg s^{-1} (Matsumoto & Tsuru 1999; Matsumoto et al. 2001; Kaaret et al. 2001). If one assumes that its luminosity is less than the Eddington luminosity (L_{Edd}), the mass of the central object must be at least $\sim 700M_{\odot}$. Hence, M82 X-1 has been considered an *intermediate* mass black hole candidate (Matsumoto et al. 1999; Kaaret et al. 2001).

However, M82 X-1 exhibits X-ray energy spectrum which is much harder than what is expected from standard accretion disks around intermediate black holes. In fact, the characteristic color temperature of the standard disk shining at the Eddington luminosity is ≈ 1 keV $(M/10 M_{\odot})^{-1/4}$, which has been confirmed through observations of many Galactic black hole candidates. Therefore, if M82 X-1 has the standard disk around an intermediate mass black hole with $\gtrsim 700M_{\odot}$, the characteristic disk temperature is expected to be $\lesssim 0.3$ keV. To the contrary, M82 X-1 indicates much harder, power-law type spectrum (e.g., Strohmayer & Mushotzky 2003; Fiorito & Titarchuk 2004; Agrawal and Misra 2006). Such apparently high disk temperatures have been also reported from other ULXs (e.g., Okada et al. 1998; Makishima et al. 2000).

There are two major models to explain the “too hot a disk” problem of M82 X-1 and other ULXs. The first model assumes that the accretion disk is not in the standard disk state where the gravitational energy released is converted into optically thick radiation, but in a *slim disk* state where radial energy advection is dominant (Watarai, Mizuno & Mineshige 2001; Mizuno, Kubota & Makishima 2001; Ebisawa et al. 2003). The competing model assumes that the ULX disks have low temperature ($\lesssim 1$ keV) as expected for intermediate mass black holes. Such disks are assumed to be shrouded by hot, Compton thick clouds, and the observed X-ray spectra above ~ 1 keV are due to inverse Compton process (approximated

by a power-law) of the seed photons from the low temperature disk (e.g., Miller et al. 2003; Miller, Fabian & Miller 2004; Fiorito & Titarchuk 2004; Wang et al. 2004).

In general, it is difficult to distinguish the two competing ULX spectral models, since these two models have similar spectral shapes in the energy range where most X-ray sensors are sensitive. In this paper, we present a precise spectral analysis of *XMM-Newton* data of M82 X-1 for a 105 ksec exposure. Thanks to the much better statistics than previous observations, we were able to tightly constrain the spectral models. We show the slim disk model can explain the M81 X-1 energy spectrum above ~ 3 keV (where contamination of star-burst component is negligible), which suggests presence of a *stellar* black hole in the center of M82 X-1.

2. Observation and Data Analysis

There are three archival *XMM-Newton* data sets of M82. Two observations were made on May 6, 2001; for 10 ksec (ObsID=0112290401) and 29 ksec (ObsID=0112290201), respectively. The other was made on April 21, 2004 for 105 ksec (ObsID=0206080101), which we analyze in the present paper. The observation was carried out employing the European Photon Imaging Camera (EPIC) PN and MOS in the full window and medium filter mode. Data screening, region selection and event extraction were performed with the standard software package XMM-SAS v 6.1.0. In order to eliminate possible contamination from solar flares, events were selected only when the total off-source count rate is less than 0.17 (MOS) and 0.55 (PN) counts s^{-1} in 10 – 15 keV. This leaves 63 (MOS1), 65 (MOS2) and 50 (PN) ksec of useful time with an average count rate of 0.7 (MOS) and 2.2 (PN) counts s^{-1} . In this paper, we will primarily analyze the PN data, which have better statistics. The MOS data gives the same results with slightly larger statistical errors.

We extracted the spectrum of M82 X-1 within a radius of $18''$ around the point source; this procedure is the same as described in Fiorito et al. (2004) and Strohmayer et al. (2003). *XMM-Newton*'s moderate spatial resolution ($13''$ – $15''$ in half power diameter) does not allow us to fully resolve the surrounding faint sources resolved by *Chandra*, including sources 4, 5, and 6 in Matsumoto et al. (2001). However, sources 4 and 6 are always at least a factor of 10 fainter than M82 X-1, and source 5 was a factor of 3.4 fainter when M82 X-1 was the faintest (Strohmayer et al. 2003). Thus, contamination from these point sources to our M82 X-1 spectral analysis is insignificant. *Chandra* also revealed diffuse emission in the central region of M82, which is obvious in the EPIC images and spectra as well. In order to concentrate on the point source spectral analysis, we limit our spectral fitting to the energy range $E > 3$ keV, where we estimate the diffuse flux less than 10 % of the point source flux.

The background spectrum was extracted from a ring of the 2' outer radius and the 18" inner radius (within which the M82 X-1 spectrum was extracted), and it was subtracted from the source spectrum after being normalized to the detector area.

The pulse-height spectral data were binned by 32 channels, which correspond to twice the energy resolution (FWHM). Fittings were performed from 3 to 11 keV using xspec v.11.3.2. We did not include the interstellar absorption model, since including of which does not affect the fitting result above 3 keV at all. First, we employed a power-law model and found that there is a weak iron emission line near 6 keV which may be modeled by a single Gaussian. The photon index is found to be 1.73. The Gaussian line is centered at 6.61 keV, and has the equivalent width 87 eV. Such an iron emission line may originate either from a disk reflection or a diffuse star-burst component, but an investigation for its origin is beyond the scope of current paper. We find χ^2 to be 96 with 43 d.o.f. Next, we applied the disk blackbody model (Mitsuda et al. 1984) to approximate a standard accretion disk (Shakura & Sunyaev 1973), including a Gaussian line with similar parameters as above. The disk blackbody temperature is found to be 2.77 ± 0.07 keV (90% confidence level for a single parameter hereafter), and $\chi^2 = 81$ (43 d.o.f.). Other fitting parameters are shown in Table 1.

Both the power-law model and the disk blackbody model are rejected with a confidence level of 99.98%. Importantly, if we compare the two model fits, we notice opposite trends in the residuals (Fig. 1). Namely, the observed spectrum is slightly “curved” downward while the power-law, of course, does not. Also, the observed curvature is not as large as that of the disk blackbody model. This indicates that the observed spectral curvature is just between that of the power-law model and the disk blackbody model.

Therefore, we then attempted the “*p-free*” disk model (Mineshige et al. 1994; Hirano et al. 1995; Kubota and Makishima 2004; Kubota et al. 2006), where the temperature profile of the accretion disk is given as $T(r) = T_{in} (r/r_{in})^{-p}$ with r_{in} , T_{in} , and p being free parameters¹. The disk blackbody model has $p = 0.75$, and a smaller p value reduces the spectral curvature and make the spectral shape closer to the power-law. We found the best fit parameters $p = 0.61_{-0.02}^{+0.03}$, $T_{in} = 3.73_{-0.40}^{+0.58}$ keV with $\chi^2 = 55$ (42 d.o.f.). The Gaussian parameters are almost the same as those of the other two models. Statistically, the *p-free* disk model describes the spectral shape best among the three models. We can calculate the *F*-value as a measure of the improvement of *p-free* model relative to the disk blackbody model. We find $F(1, 42) = \Delta\chi^2/\chi^2_{\nu} = (81 - 55)/(55/42) = 19.9$. Thus, the improvement of the *p-free* model over the disk blackbody model is significant with the 99.99 % confidence.

¹This model is now available in the standard xspec v.12.3.0 or later with the name “diskpbb”.

When the disk luminosity is as high as the Eddington luminosity, an optically-thick Advection Dominated Accretion Flow (ADAF) appears (Abramowicz et al. 1988). Such a flow, often called a *slim disk*, has very low radiation production efficiency due to photon trapping (Begelman 1978). The low energy spectrum of the slim disk has the form $L_E \propto E^{-1}$ (Fukue 2000), while that of the standard disk is $L_E \propto E^{0.33}$. Since the disk spectral shape is related to the radial exponent p as $L_E \propto E^{3-2/p}$, the spectral change from the standard disk to the slim disk is equivalent to the reduction of p from 0.75 to 0.5 (Watarai et al. 2000).

Our result of $p = 0.61_{-0.02}^{+0.03}$ strongly suggests that energy advection is actually taking place, and that the M82 X-1 disk is not in the standard state, but in a slim disk state. In this paper, we employ our own slim disk model² (Kawaguchi 2003) to study M82 X-1 energy spectrum. Kawaguchi (2003) has calculated slim disk spectra under four different assumptions. In Model 1, the local emission is assumed to be modified blackbody, and in Model 2, Comptonization is taken into account. Gravitational redshift is included in Model 3; and in Model 4, which is our “best” model, transverse Doppler effects are additionally considered. In Figure 2, we compare the simulated Model 4 spectrum with power-law, disk blackbody, and p -free disk model. It is obvious that the simulated Model 4 spectral shape is well-represented by the p -free model, and its curvature is just between those of the power-law and disk blackbody. Comparing Figure 1 and 2, we can see that M82 X-1 and the simulated Model 4 share similar spectral characteristics.

Next, we directly fit the M82 X-1 spectrum with our slim disk model. We try all four models with assumptions as listed in Table 1. We tried models with the viscous parameter $\alpha = 0.001, 0.01, 0.1$ and 1, and found that $\alpha = 1$ gives the best-fit. We also fit allowing α to be free, with little improvement of the fit. Thus, we show only the results with $\alpha = 1$ in Table 1. Fixing the distance to M82 at 2.7 Mpc (e.g., Rieke et al. 1980), there are then only two free parameters, M and \dot{M} . Kawaguchi’s model calculates the face-on disk flux, so we assume the face-on geometry in the following.

As summarized in table 1, we obtain $M = (19 - 32) M_\odot$, $\dot{M} = (320 - 560) \times L_{\text{Edd}}/c^2$ depending on the physical processes assumed. In the case of the standard optically thick accretion disk where the inner disk radius is three times the Schwarzschild radius, $\dot{M} = 17.5 L_{\text{Edd}}/c^2$ gives the Eddington luminosity; so we can see that M82 X-1 has extremely high mass accretion rates. However, since slim disks are radiation inefficient, the disk luminosity is not so large as being proportional to the mass accretion rates. Bolometric face-on flux f_{bol} is obtained as $\sim 3 \times 10^{-11} \text{ erg s}^{-1} \text{ cm}^{-2}$ by numerically integrating the best-fit model

²This model is available at <http://heasarc.gsfc.nasa.gov/docs/xanadu/xspec/models/slimdisk.html> for use in xspec

spectra over the energy, which is weakly dependent on the assumptions. The bolometric disk luminosity is $L_{bol} = 2\pi d^2 f_{bol}$ where d is the distance (2.8 Mpc), and we obtain $L_{bol} \approx 1.4 \times 10^{40}$ erg s⁻¹. Hence, depending on the assumptions, our slim disk model fits suggest that M82 X-1 is shining at 4 to 6 times the super-Eddington luminosity.

3. Discussion

We have studied the M82 X-1 spectrum using archival *XMM-Newton* data of 105 ksec exposure. We have applied the slim disk spectral model of Kawaguchi (2003), and estimated the mass $M \approx (19 - 32) M_{\odot}$ and the bolometric luminosity 4 to 6 times the Eddington luminosity. Since ULXs are, by definition, very luminous objects, it is rather straightforward that their accretion disks are in the slim disk state, rather than the standard state. While standard accretion disks around $\gtrsim 20 M_{\odot}$ black holes have characteristic temperatures $\lesssim 0.8$ keV (see Section 1), slim disks can explain the observed high disk temperature (~ 2.8 keV).

We briefly review why a slim disk can produce such a hard spectrum (see Kawaguchi 2003 for more detail). (1) As the mass accretion rate increases, the innermost radius of the slim disk can be smaller than three times the Schwarzschild radius even in the Schwarzschild geometry (Watarai et al. 2000), which makes the innermost disk temperature higher. (2) The ratio of the electron scattering opacity to the absorption opacity increases with mass accretion rates. Thus, photons generated deeper in the disk, where the temperature is higher, can escape from the disk surface more easily, and the local spectral shape gets closer to modified blackbody, rather than the standard blackbody (e.g., Rybicki & Lightman 1979). (3) Furthermore, because of the small absorption, inverse Compton scattering (disk Comptonization) is enhanced to shift energies from electrons to emerging photons. Above (1) increases the disk effective temperature, while (2) and (3) increases the spectral hardening factor which is ratio of the local color temperature and the effective temperature.

Based on the slim disk model fitting, we have found M82 X-1 is shining at 4 to 6 times the Eddington luminosity. Although the standard disk cannot exceed the Eddington limit, such a moderate super-Eddington luminosity is naturally explained in the slim disk model (e.g., Abramowicz et al. 1988; Watarai et al. 2000). Also, a recent two-dimensional radiation-hydrodynamic numerical simulation reports that a slim disk is formed under supercritical accretion flow, and the disk luminosity can exceed the Eddington luminosity by several factors (Ohsuga et al. 2005).

We have estimated the black hole mass in M82 X-1 as $\approx 19 - 32 M_{\odot}$. Although we have not seen such a rather heavy stellar-mass black hole in our Galaxy, such black holes are not

prohibited by stellar evolution theory (e.g., Fryer 1999). Actually, a universal luminosity function for X-ray binaries extends toward the highest luminosity $\sim 10^{40}$ erg s $^{-1}$ without any break (Grimm, Gilfanov & Sunyaev 2003), and it is likely that ULXs correspond to the highest luminosity X-ray binaries. This scenario agrees with the binary evolution synthesis model of ULXs by Rappaport, Podsiadlowski & Pfahl (2005), which strongly suggests ULXs are stellar-mass black hole binaries. Finally, detailed evolution models of stellar binaries show very small generation rate of intermediate-mass black holes (Madhusudhan et al. 2006), which is also in favor of our stellar-mass ULX model.

In conclusion, we suggest that the brightest ULX M82 X-1 harbors a rather heavy but still stellar-mass black hole shining at several times the Eddington luminosity. The slim disk model is reasonably successful in explaining the X-ray energy spectrum of M82 X-1 above ~ 3 keV. The high disk luminosity and temperature, which are characteristics of the slim disk, are not specific to M82 X-1, but also seen from some other ULXs. We propose that those ULXs having similar disk properties may also be interpreted in the framework of the slim disk model with stellar black holes shining at super-Eddington luminosities.

Finally, we remark that the present data analysis of M82 X-1 was limited above ~ 3 keV in order to avoid contamination from the soft star-burst component, whereas the disk spectra from putative “intermediate-mass black holes” would be most prominent below ~ 3 keV. Therefore, it will be interesting to apply our slim disk scenario to other ULXs in which their disk spectra are clearly seen below 3 keV as well as above 3 keV. If the slim disk model is successful to explain the ULX energy spectra in the entire energy range, intermediate-mass black holes are not required to explain the X-ray energy spectra of ULXs.

TO acknowledges support from NASA Grant NNG04GB78A. TK thanks the financial supports from the Japan Society for the Promotion of Science (JSPS) Postdoctoral Fellowships. This research has made use of public data and software obtained from the *XMM-Newton* Science Archive (XSA), provided by the European Space Agency (ESA), and the High Energy Astrophysics Science Archive Research Center (HEASARC), provided by NASA’s Goddard Space Flight Center. The authors thank John P. Lehan for useful comments and assistance in correcting grammatical errors in the manuscript.

REFERENCES

- Abramowicz, M. A., Czerny, B., Lasota, J. P., & Szuszkiewicz, E., 1988, ApJ, 332, 646
- Agrawal, V. K. & Misra, R. 2006, ApJ, 638, L83

- Begelman M.C. 1978, MNRAS, 184, 53
- Ebisawa, K., Życki, P., Kubota, A., Mizuno, T. & Watarai, K. 2003, ApJ, 597, 780
- Fiorito, R., & Titarchuk, L., 2004, ApJ, 614, L113
- Fukue. J, 2000, PASJ, 52, 829
- Fryer. C. L., 1999, ApJ, 522, 413
- Grimm, H. J., Gilfanov, M., & Sunyaev, R., 2003, MNRAS, 339, 793
- Hirano, A., Kitamoto, S., Yamada, T., Mineshige, S. & Fukue, J. 1995, ApJ, 446, 350
- Kaaret, P., Prestwich, A. H., Zezas, A., Murray, S. S., Kim, D.-W., Kilgard, R. E., Schlegel, E. M., & Ward, M. J., 2001, MNRAS, 321, L29
- Kawaguchi T., 2003, ApJ, 593, 69
- Kawaguchi T., 2004, Porg. Theor. Phys. Suppl., 155, 120
- Kubota, A., Ebisawa, K., Makishima, K. & Nakazawa, K. 2005, ApJ, 631, 1062
- Madhusudhan N. et al. 2006, ApJ, 640, 918
- Matsumoto, H., Tsuru, T. G., Koyama, K., Awaki, H., Canizares, C. R., Kawai, N., Matsushita, S., & Kawabe, R., 2001, ApJ, 547, L25
- Matsumoto, H., & Tsuru, T. G. 1999, PASJ, 51, 321
- Makishima, K. et al. 2000, ApJ, 535, 632
- Mitsuda, K., Inoue, H., Koyama, K., Makishima, K., Matsuoka, M., Ogawara, Y., Suzuki, K., Tanaka, Y., Shibazaki, N., & Hirano, T., 1984, PASJ, 36, 741
- Miller, J. M., Fabian, A. C. & Miller, M. C. 2004, ApJ, 607, 931
- Miller, J. M., Fabbiano, G., Miller, M. C. & Fabian, A. C. 2003, ApJ, 585, L37
- Mineshige, S., Hirano, A., Kitamoto, S., Yamada, T., & Fukue, J., 1994, ApJ, 426, 308
- Mizuno, T., Kubota, A & Makishima, K. 2001, ApJ, 554, 1281
- Ohsuga, K. et al. 2005, ApJ, 628, 368
- Okada, K. et al. 1998, PASJ, 50, 25

Ptak, A., & Colbert, E. 2004, ApJ, 606, 291

Rieke, G. H. et al. 1980, ApJ, 238, 24

Rybicki, G. B., & Lightman, A. P. 1979, Radiative Processes in Astrophysics, John Willey & Sons, New York

Strohmayer, T. E., & Mushotzky, R. F., 2003, ApJ, 586, L61

Shakura, N. I., & Sunyaev, R. A. 1973, A&A, 24, 337

Rappaport, S. A., Padsiadlowski, Ph., & Pfahl, E., 2005, MNRAS, 356, 401

Wang, Q. D., Yao, Y., Fukui, W., Zhang, S. N. & Williams, R. 2004, ApJ, 609, 113

Watarai, K., Mizuno, T. & Mineshige, S. 2001, ApJ, 549, L77

Watarai, K., Fukue, J., Takeuchi, M. & Mineshige, S. 2000, PASJ, 52, 133

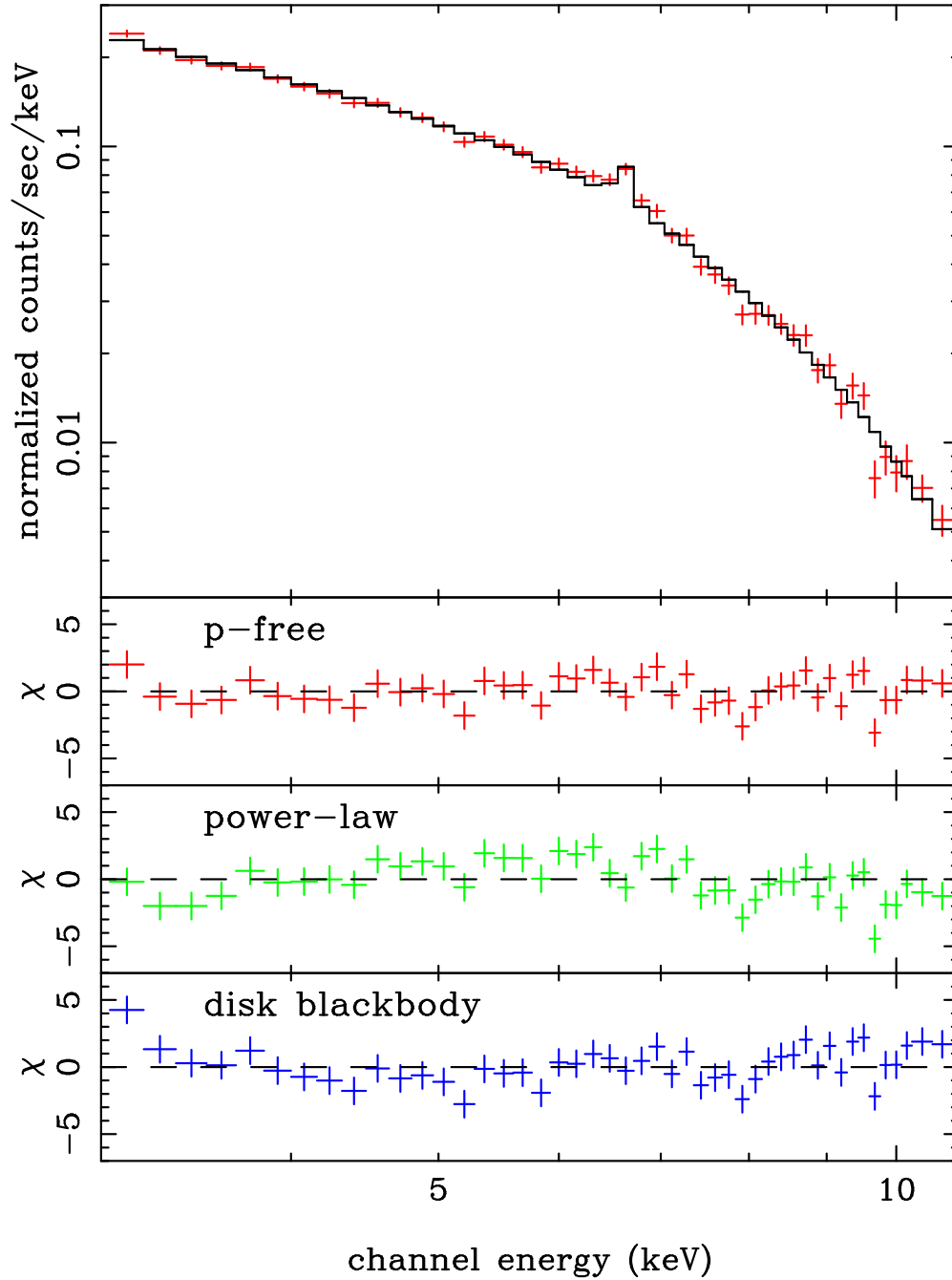


Fig. 1.— Folded spectrum of M82 X-1, fitted with the p -free disk blackbody and narrow Gaussian model (top), and residuals for fitting with three different models, p -free, power-law, and disk blackbody.

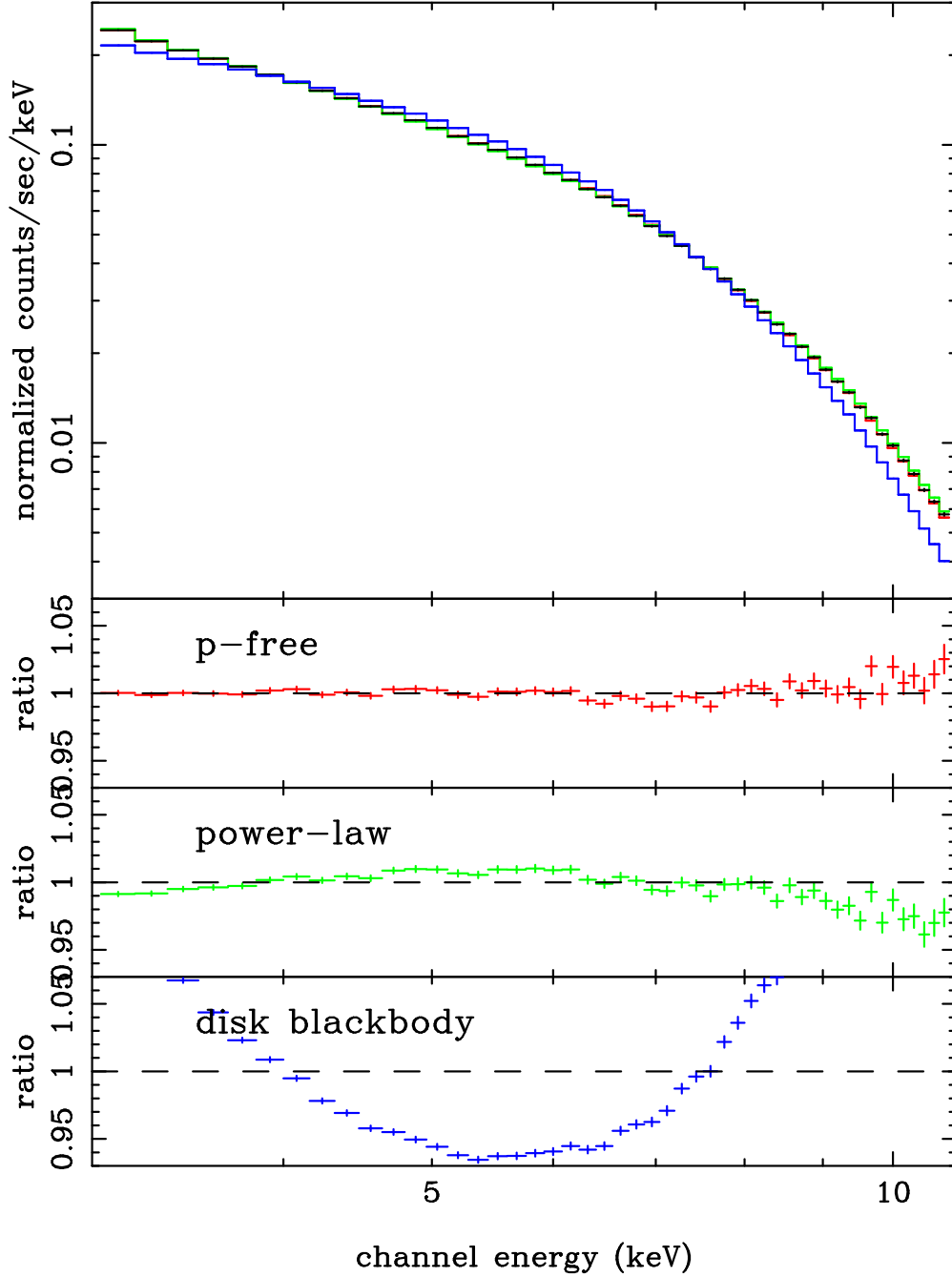


Fig. 2.— Comparison of the slim disk model by Kawaguchi (2003) and other models used to fit M82 X-1. A simulated spectrum was made from Kawaguchi’s model 4 (see text) with $\alpha = 1$, $M = 30M_{\odot}$ and $\dot{M} = 350 L_{Edd}/c^2$ at 2.7 Mpc, and fitted with a power-law (index=1.76), disk blackbody ($T_{in} = 2.72$), and p -free disk model ($p = 0.54$ and $T_{in} = 7.60$). The top panel shows the simulated slim disk spectrum and the best-fit models, and the three bottom panels exhibit the ratios of the simulated data to the p -free model, power-law and disk blackbody, respectively. Note that slim disk (solid line) and p -free (dashed line) models are almost identical.

Table 1. Fitting parameters

model name	continuum model parameters				Gaussian model ^a		$\chi^2/\text{d.o.f.}$	
	Γ	T_{in} (keV)	p	N	E (keV)	EW (eV)		
power-law	1.73	0.00292 ^b	6.61	87.1	96/43*	
disk blackbody	...	2.77 ± 0.07	0.75	0.0130 ^c	$6.63^{+0.06}_{-0.05}$	61^{+23}_{-18}	81/43	
p -free	...	$3.73^{+0.58}_{-0.40}$ keV	$0.61^{+0.03}_{-0.02}$	$0.0028^{+0.0017}_{-0.0014}$ ^c	$6.62^{+0.06}_{-0.04}$	72^{+23}_{-20}	55/42	
slim disk ($\alpha = 1$) ^d	Local Spectral Assumption			M/M_{\odot}	$\dot{M}/(L_{\text{Edd}}/c^2)$			
1	modified B.B. ^e			19	395	6.61	85	91/43*
2	Comptonization ^f			19	559	6.61	85	88/43*
3	Comptonization+gravitational redshift ^g			27^{+9}_{-4}	366^{+100}_{-190}	$6.61^{+0.07}_{-0.03}$	86^{+11}_{-22}	85/43
4	Comptonization+relativistic effects ^h			32^{+6}_{-5}	320^{+60}_{-140}	$6.61^{+0.07}_{-0.03}$	86 ± 21	84/43

Note. — Errors correspond to the single parameter 90 % confidence.

^aIntrinsic line-width is fixed to 0.01 keV

^bNormalization at 1 keV (photons $\text{s}^{-1} \text{keV}^{-1} \text{cm}^{-2}$).

^c $((R_{in}/1 \text{ km})/(d/10 \text{ kpc}))^2 \cos \theta$ where d is the distance, R_{in} is the innermost disk radius and θ is the inclination.

^dSource distance is fixed at 2.7 Mpc.

^eLocal emission at each radius is computed considering electron scattering opacity. See §3.

^fLocal emission at each radius is computed considering Compton effects.

^gGravitational redshift is included.

^hIn addition to gravitational redshift, the transverse Doppler effect is included.

*Errors are not derived because reduced $\chi^2 > 2$.